

Physicochemical studies on turnip-yellow-mosaic virus

Homogeneity, relative molecular masses, hydrodynamic radii and concentration-dependence of parameters in non-dissociating solvents

Stephen E. HARDING* and Paley JOHNSON†

Department of Biochemistry, University of Cambridge, Tennis Court Road, Cambridge CB2 1QW, U.K.

Turnip-yellow-mosaic virus, with its stable, highly spherical and monodisperse character, was chosen as a suitable model substance with which to test hydrodynamic theories of transport. Sedimentation coefficients, diffusion coefficients (obtained through photon correlation spectroscopy) and viscosities were measured accurately as a function of concentration in well-defined and nearly neutral buffer systems. Ancillary information was also obtained from very-low-speed sedimentation-equilibrium experiments. The coefficients expressing the variation in sedimentation and diffusion coefficients with weight concentration were obtained, and by combination with other data it was possible to avoid assumptions concerning solvation and transform such regression coefficients into the form appropriate to volume fractions. Some measure of support for Batchelor's [(1972) *J. Fluid Mech.* **52**, 245–268] calculations was thus obtained, but over most of the pH range the coefficients were significantly smaller than those calculated from his theory. It seems likely that electrostatic interactions are responsible for the discrepancies. Hydrodynamic radii (from diffusion coefficients) were in very fair agreement with those calculated from the thermodynamic excluded-volume term, but were higher than indicated by electron microscopy and X-ray diffraction, a discrepancy ascribable to solvation.

INTRODUCTION

Turnip-yellow-mosaic (TYM) virus has been characterized both hydrodynamically (Markham, 1951; Kaper, 1960*a, b*, 1975) and by electron microscopy (Klug & Finch, 1960). The work of Markham (1951) and of Klug & Finch (1960) showed that the virus consisted of an essentially spherical protein shell that encased the RNA. A proportion of the virus as normally prepared was found not to contain RNA and hence to be non-infective, although the protein shell retained the same conformation as the intact virus. Kaper (1960*b*) has shown that it was possible to obtain such 'top components' artificially by controlled exposure of the intact virus to strongly alkaline conditions (pH 12). Prolonged exposure resulted in the irreversible dissociation of the protein shell into subunits.

In work involving the use of photon correlation spectroscopy as well as sedimentation velocity (Godfrey *et al.*, 1982), the concentration-dependences of the diffusion and sedimentation coefficients were shown not to be in agreement with previous work. Since such matters are of importance in solution theory, a comprehensive re-examination has been undertaken, with the use of, additionally, sedimentation-equilibrium and viscosity measurements. TYM virus has the great advantage of being spherical, though without a smooth surface, and, unlike many latex preparations, can be highly monodisperse in dilute solution. Further, TYM-virus particles are small enough to ensure overwhelming Brownian motion; their only disadvantage as compared with latex particles lies in their solvation capacity.

MATERIALS AND METHODS

Solvents

Four phosphate buffers were used as solvents: (i) pH 7.8, *I* 0.10; (ii) pH 6.8, *I* 0.10; (iii) pH 6.0, *I* 0.10; (iv) pH 6.8, *I* 0.20. The relevant proportions of Na₂HPO₄ and KH₂PO₄ were made up to a combined ionic strength of 0.05, and the higher ionic strengths (0.10, 0.20) were attained by adding relevant proportions of NaCl in accordance with Green (1933).

In addition, one acetate buffer was used, made up to a pH of 4.75 and an ionic strength of 0.10 in accordance with Dawson *et al.* (1969).

TYM virus

TYM virus (generously given by Dr. P. Witz, University of Strasbourg, Strasbourg, France) was stored below 0 °C in 50% (w/w) glycerol. Samples were dialysed extensively against distilled water at 4 °C to remove glycerol and then finally against an appropriate solvent. They were then examined by sedimentation velocity to check for significant contamination by 'top component', which was less than 1% for all samples (e.g. see Fig. 1).

Diffusion-coefficient measurements: photon correlation spectroscopy

The apparatus was essentially that as described previously (Godfrey *et al.*, 1982; Harding & Johnson, 1984) except for modifications of the light-scattering housing to allow measurements at an angle as low as 5°. Two alternative light sources were used: a 15 mW He/Ne

Abbreviation used: TYM virus, turnip-yellow-mosaic virus.

* Present address: Department of Applied Biochemistry and Food Science, University of Nottingham, School of Agriculture, Sutton Bonington, Loughborough LE12 5RD, U.K.

† Present address: Cavendish Laboratory, University of Cambridge, Madingley Road, Cambridge CB3 0HE, U.K.

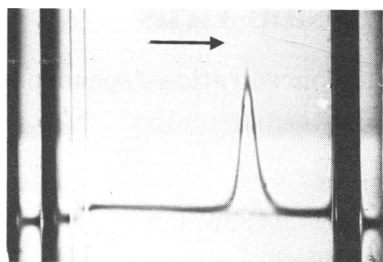


Fig. 1. Sedimentation diagram of TYM virus solution in phosphate/NaCl buffer

Sedimentation was at 14290 rev./min (c 4.50 mg/ml, pH 6.8, I 0.20), in a 12 mm double-sector cell. The phase-plate angle was 45° .

laser (Spectra Physics) with wavelength (λ) of 632.8 nm, and a PSL air-cooled (model 82) argon-ion laser with output adjustable up to 60 mW. The latter laser had been fitted with an intensity-feedback mechanism to assist in the constancy of the power output, and its prism was adjusted to a wavelength of 488.0 nm.

The beam from either laser was focused on to the centre of a 1 cm \times 1 cm cuvette. The cuvette was placed at the centre of a goniometer so that the scattering angle could be varied from 5° to 90° . As previously observed for TYM virus, diffusion coefficients showed no trend with changing angle, so that an angle of 90° was normally utilized. Stray light was decreased by a series of 'baffles', which screen off the path of the incident and emergent beams from the collecting system. The scattered light was collected (homodyne collection) by well-collimated pin holes to reach an EMI 9863 photomultiplier. Output from the multiplier was led to a Malvern Amplifier Discriminator (RR63), which gave output pulses of width 30 ns and -2 V amplitude, suitable for processing in a 128-channel Malvern Correlator (K7025). The non-normalized correlation function products were displayed against channel number (or time) on an oscilloscope. Digital output from the correlator was directed via the memory of a BBC microcomputer on to a floppy disc, each side of which could store 30 runs. Data could then be passed back via the microcomputer to the main university IBM/3081B computer for processing. The routine used produced an accurate plot of $\ln[g^2(t) - 1]$ versus time, t , where $g^2(t)$ is the normalized intensity correlation function. z -average diffusion coefficients were obtained from the limiting slope (see, e.g., Pusey, 1974). The routine produced the best least-squares fit of this plot to a linear, quadratic or cubic polynomial, and a guide to the best fit was provided by the ϵ function (see, e.g., Teller, 1973, p. 375). The routine also calculated the 'polydispersity factor', namely the z -averaged normalized variance of the distribution of the diffusion coefficients (Pusey, 1974).

Diffusion coefficients, D_c , at a given concentration, c , in a particular buffer b at an absolute temperature T , were normalized to standard conditions (water as a solvent at 20°C) according to the usual formula:

$$D_{c(20,w)} = \frac{293.15}{T} \cdot \frac{\eta_{T,b}}{\eta_{20,w}} \cdot D_c(T,b) \quad (1)$$

where $\eta_{T,b}$ is the solvent viscosity at temperature T and $\eta_{20,w}$ the viscosity of water at 20°C . In all that follows

we use the symbol D_c in place of $D_{c(20,w)}$ and D as the value of the D_c values extrapolated to infinite dilution.

Cleaning of cells and clarification of solutions for photon correlation spectroscopy

The cleaning and clarification procedures were essentially as previously described (Godfrey *et al.*, 1982). Each cell was repeatedly flushed with ultrafiltered water by using a filling apparatus similar to that described by Sanders & Cannell (1980), and dried with ultrafiltered air. A TYM virus solution was then introduced into the cell through the same Millipore (type HA, $0.45 \mu\text{m}$ pore size) filter and hypodermic needle.

Concentration measurements

Concentrations of TYM virus solutions were determined spectrophotometrically with 1 mm-pathlength cells. An absorption coefficient of $8.6 \times 10^3 \text{ litre} \cdot \text{g}^{-1} \cdot \text{cm}^{-1}$ at 260 nm (Kaper & Litjens, 1966) was used. Concentrations for the diffusion measurements were measured after filtration.

Sedimentation-coefficient measurements

A Spinco model E analytical ultracentrifuge was used with an RTIC temperature-measurement system, which was calibrated regularly. Schlieren optics were mainly employed. In general, single symmetrical boundaries were observed (although such symmetry is not in itself proof of homogeneity), with occasionally evidence for a very small amount ($< 1\%$) of tailing 'top component' (Markham, 1951). Linear plots of $\ln r$ versus t were obtained, where r is the radial distance of the position of maximum refractive-index gradient. Eight to 12 frames were used in determining each value of s_c .

Sedimentation coefficients are normally corrected to standard conditions (water as solvent at 20°C) by using the usual formula:

$$s_{c(20,w)} = \frac{(1 - \bar{v}\rho_{20,w}) \cdot \eta_{T,b}}{(1 - \bar{v}\rho_{T,b}) \cdot \eta_{20,w}} \cdot s_{c(T,b)} \quad (2)$$

Here \bar{v} is the partial specific volume, ρ refers to the solution density and $\eta_{T,b}$ to the solvent viscosity. In all that follows the symbol s_c is used in place of $s_{c(20,w)}$. Use of solution densities for each concentration is rather difficult, tedious and wasteful of material, and so we follow the common procedure of using solvent densities. This has no effect on the value of s_c extrapolated to infinite dilution (s), and a simple correction is available for the concentration-dependence regression factor k_s [see eqn. (9) below]. In addition, values of the regression parameter had already been corrected for radial dilution.

Sedimentation-equilibrium measurements

A Beckman model E analytical ultracentrifuge was used, similar to the earlier model described above except for the electronically controlled drive. Rayleigh-interference optics were used. Because of the high relative molecular mass ('molecular weight') of the particle (5.5×10^6), a low equilibrium speed (2000 rev./min) was used to ensure adequate resolution of the fringes near the cell base. Even at this speed, near meniscus-depletion conditions were obtained. Nonetheless the meniscus concentration remained measurable and was obtained by mathematical manipulations of the fringe data (see, e.g., Creeth & Harding, 1982a) and also by the synthetic-boundary method of monitoring fringe movement at the

meniscus (see Nureddin & Johnson, 1977). The two methods agreed to better than one-tenth of a fringe. Point weight-average apparent relative molecular masses, $M_{w(\text{app.})}$, were obtained by employing sliding-strip quadratic fits to the observed fringe data. Estimates for the 'ideal' weight-average relative molecular mass, M_w , and the second virial coefficient B were obtained from plots of $1/M_{w(\text{app.})}$ against concentration, the slope being $(1/M_w)(2BM_w - \bar{v})$ (see, e.g., Ross & Minton, 1977). Absolute concentrations were also obtained from fringe concentrations for this procedure, as normally, by using the synthetic-boundary cell. Whole-cell weight-average relative molecular masses, M_w^{cell} , were extracted by using the limiting value at the cell base of a directly determinable point average (Creeth & Harding, 1982a); an independent estimate for the initial concentration was not required. Cells of 12 mm pathlength were used, except when checking for homogeneity, when 12 mm-pathlength and 30 mm-pathlength cells were used simultaneously.

Intrinsic-viscosity determination

Sufficient material was available for the determination of an approximate value for the intrinsic viscosity at pH 6.8 and $I 0.10$. Flow times of solutions and solvent were determined in an Ostwald-type viscometer (capacity 2 ml) suspended reproducibly in a bath thermostatically maintained at 25.00 ± 0.01 °C. Kinematic viscosities were obtained from the ratio of the flow times for solution and solvent, and the kinematic intrinsic viscosity $[\eta']$ (ml/g) was obtained from the extrapolation of the (kinematic) reduced specific viscosity to zero solute concentration. The dynamic intrinsic viscosity $[\eta]$ was obtained from $[\eta']$ by using the correction factor of Tanford (1955a):

$$[\eta] = \frac{1 - \bar{v}\rho_0}{\rho_0} + [\eta'] \quad (3)$$

where ρ_0 is the density of the solvent. Glycerol (3%) was included in the solvent before dialysis; this enabled viscosities to be determined at a concentration of 4.10 mg/ml and lower without problems of wall effects (Szuchet-Derechin & Johnson, 1966).

Isoelectric-point determination

The isoelectric point was measured by using a procedure modified from that of Tanford (1955b). A cell was constructed so that the pH of a solution containing 12.8 mg of TYM virus in 1 ml of glass-distilled water in the presence of mixed-bed ion-exchange resin could be measured. N_2 was passed over the solution to avoid the effects of dissolved O_2 and CO_2 . The value for the isoelectric pH (pI) of 4.75 ± 0.05 obtained in this way differs from the value quoted by Markham (1951) of 3.75; no details were given by Markham (1951) concerning the method of measurement. It is surprising to note that Markham (1951) quoted the same value both for complete virus and 'top component'. In the present study the pH-meter had been calibrated with 0.05 M-potassium hydrogen phthalate (pH 4.001 at 20.0 °C) immediately before the measurement on the TYM virus solution.

RESULTS AND DISCUSSION

It is well known that neither a single symmetrical schlieren peak in a sedimentation-velocity experiment nor linearity of a plot of the logarithm of fringe concentration versus radial displacement in sedimentation-

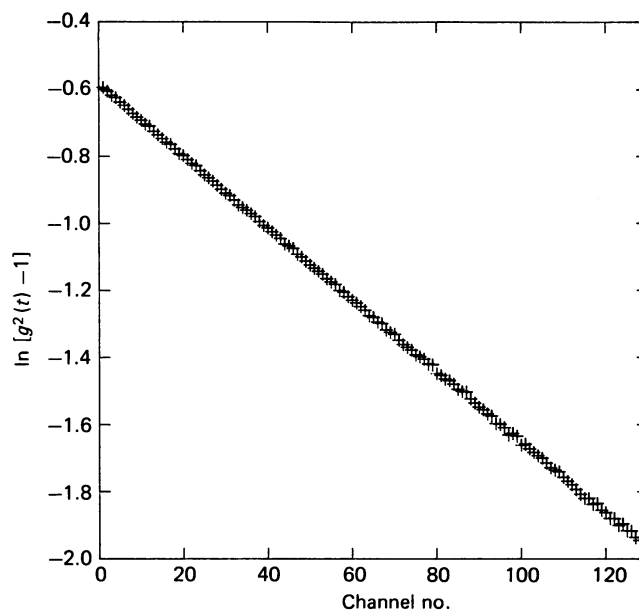


Fig. 2. Plot of $\ln[g^2(t) - 1]$ as a function of channel number for TYM virus in phosphate/NaCl buffer at pH 4.75 and $I 0.10$

The scattering angle, θ , was 90° and the sample time was $1.0 \mu\text{s}$. The duration time was 60 s. The temperature was 24.85 °C. $c = 4.07$ mg/ml.

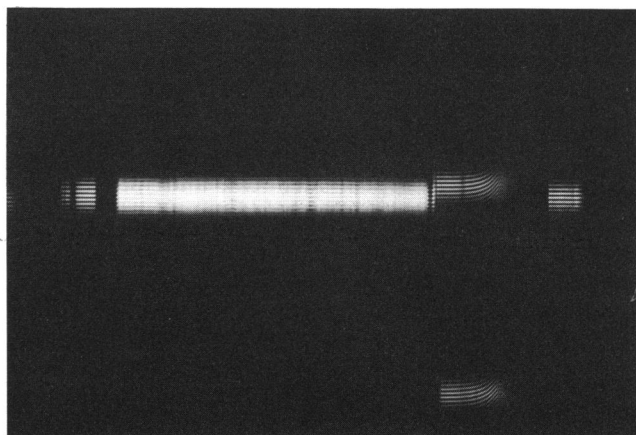


Fig. 3. Homogeneity experiment on TYM virus solution in acetate buffer

Rayleigh-interference optics were used. The solution was at pH 4.75 and $I 0.10$. The rotor speed was 2000 rev./min, and the temperature was 15.8 °C. Upper pattern: 30 mm cell, $c^0 = 0.41$ mg/ml. Lower pattern: 12 mm cell, $c^0 = 1.02$ mg/ml.

equilibrium experiments is a sufficient criterion for the homogeneity of a preparation. However, in the present case of a highly purified crystalline virus, the only likely impurities were 'top component' and possible aggregation products. In the worst case, less than 1% of a 'top-component' peak was observed, with no signs of aggregation product. In addition, plots of the logarithm of the normalized correlation function {strictly $\ln[g^2(t) - 1]$ } versus channel number in the diffusion

Table 1. Hydrodynamic and thermodynamic parameters for TYM virus in various non-dissociating solvent conditions

Symbols are as defined in the text. Ionic strength was 0.10 except where indicated by an asterisk (*), when it was 0.20.

pH	$10^{13} \times s$ (s^{-1})	$10^7 \times D$ ($cm^2 \cdot s^{-1}$) ($\pm 0.05 \times 10^{-6}$)	$10^{-6} \times M_w$ ($\pm 0.2 \times 10^{-6}$)	$10^{-6} \times M_w^\dagger$ ($\pm 0.2 \times 10^{-6}$)	$10^{-6} \times M_w^{cell\dagger}$ ($\pm 0.2 \times 10^{-6}$)	k_D (± 0.10) (ml/g)	k'_s (± 0.20) (ml/g)	k_s (± 0.20) (ml/g)	$10^6 \times B$ ($\pm 0.10 \times 10^6$) (ml \cdot mol \cdot g $^{-2}$)	$10^6 \times B^\dagger$ ($\pm 0.4 \times 10^6$) (ml \cdot mol \cdot g $^{-2}$)	v_s (± 0.20) (ml/g)
7.8	115.20	1.422	5.80	5.5	5.3	3.18	11.84	11.18	1.30	1.3	1.88
6.8	113.79	1.422	5.73	5.8	5.5	5.25	8.66	8.00	1.21	1.5	1.74
6.0	113.07	1.409	5.75	5.6	5.6	5.88	9.14	8.48	1.25	1.3	1.80
4.75	111.62	1.385	5.77	5.6	5.6	4.21	8.47	7.81	1.10	1.3	1.59
6.8*	113.02	1.437	5.64	5.7	5.5	5.01	9.82	9.16	1.32	1.7	1.86

† Determined from sedimentation equilibrium; the remainder were determined from sedimentation velocity and diffusion.

experiments were all virtually linear with low polydispersity factors (< 0.04), confirming the monodispersity of the solutions (see, e.g., Fig. 2). Use has been made of a simple check on homogeneity by using sedimentation equilibrium (Creeth & Harding, 1982*b*). For this particular case two cells were used with their respective balance cells in a four-hole rotor. Typical interference-fringe representations of solute distributions for one particular preparation are shown in Fig. 3. The top pattern corresponds to a solution of initial loading concentration (c^0), 0.41 mg/ml, in a 30 mm-pathlength cell. The lower fringe pattern corresponds to the solution in a 12 mm cell (with wedge centrepiece) but a 2.5-fold higher c^0 (1.02 mg/ml) so that the initial 'fringe' loading concentrations are the same. An ideal single-solute system would give identical fringe patterns and hence identical cell weight-average relative molecular masses (M_w^{cell}). For the case shown (pH 4.75) it is seen that the fringe distributions appear identical, and indeed their M_w^{cell} values are virtually identical ($5.8 \times 10^6 \pm 0.2 \times 10^6$). It is reasonable to conclude that the samples are essentially homogeneous and thermodynamically almost ideal. A similar agreement was obtained for samples at pH 6.8 ($I 0.10$) from a different preparation (30 mm cell, $c^0 = 0.24$ mg/ml, $M_w^{cell} = 5.5 \times 10^6 \pm 0.2 \times 10^6$; 12 mm cell, $c^0 = 0.59$ mg/ml, $M_w^{cell} = 5.4 \times 10^6 \pm 0.2 \times 10^6$). The slightly lower value for the 12 mm cell (if significant) is probably indicative of the greater effect of thermodynamic non-ideality at the higher concentration.

Relative molecular masses and hydrodynamic radii of TYM virus under various solvent conditions

Relative molecular masses were determined from the sedimentation and diffusion coefficients [after correction to standard conditions (water at 20 °C) and extrapolation to infinite dilution] by using the Svedberg equation (Svedberg & Pedersen, 1940):

$$M_w = \frac{RTs}{D(1 - \bar{v}\rho)} \quad (4)$$

where \bar{v} , the partial specific volume, has the value 0.661 ml/g (Kaper & Litjens, 1966; J. M. Kaper, D. W. Kupke, D. V. Ulrich & F. N. Weber, Jr., personal communication) (assumed essentially invariant under the solvent conditions studied), and T is the absolute temperature (293.15 K).

Table 1 gives a comparison of the values of the

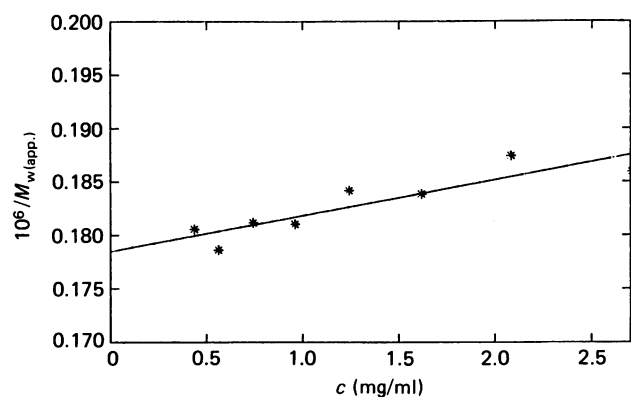


Fig. 4. Plot of the reciprocal of the apparent weight-average relative molecular mass versus concentration for TYM virus in phosphate/NaCl buffer, pH 6.8 and $I 0.20$

The rotor speed was 2000 rev./min, and the temperature was 19.00 °C. $c^0 = 0.59$ mg/ml.

Table 2. Comparison of hydrodynamic (r_H) and thermodynamic (r_B) radii for TYM virus in various solvents

pH	r_H (± 0.2) (nm)	r_B (± 1.5) (nm)
7.8	15.1	16.3
6.8	15.1	15.8
6.0	15.2	15.9
4.75†	15.5	15.4
6.8*	14.9	16.1

weight-average relative molecular mass from sedimentation/diffusion and sedimentation equilibrium under the various solvent conditions. Two types of relative molecular mass from sedimentation equilibrium are given. One (M_w) is obtained from the point weight-average apparent relative molecular mass (i.e. at a particular concentration) extrapolated to zero concentration (i.e. corresponding to 'ideal' solution conditions, as in Fig. 4).

The other (M_w^{cell}) is the whole-cell weight-average value, and is obtained by extrapolation of the star point-average relative molecular mass (M^*) to the cell base (Creeth & Harding, 1982a). In general, $M_w^{cell} < M_w$ for the present system because the effects of thermodynamic non-ideality at a finite concentration tend to lower the whole-cell weight-average value.

No discernible trend in relative molecular mass is evident as a function of pH, although it may be noted that there is a slight increase in both s and D with increase in pH. The value for D at pH 6.8 and 10.20 is about 1% higher than that for the same pH at 10.10, with a corresponding decrease in M_w . This slight decrease may represent some suppression of charge effects or a slight change in the \bar{v} . It may also be noted that the relative molecular mass calculated on the basis of amino acid sequence information and RNA content is 5.55×10^6 (Kaper, 1975; Rossman, 1984).

The hydrodynamic radius, r_H , of TYM-virus particles was calculated from the simple Einstein equation:

$$r_H = \frac{kT}{6\pi\eta D} \quad (5)$$

In Table 2 we also give these radii under different solvent conditions. The values given in this Table (≈ 15.2 nm) are significantly higher than those calculated from electron microscopy (≈ 13.5 nm; Finch & Klug, 1966) or X-ray crystallography (≈ 14.0 nm; Klug *et al.*, 1966), probably indicative of solvation effects.

Concentration-dependence parameters

Solutions of the near-spherical TYM-virus particles provide a useful system for comparing the different theories for the concentration-dependence of sedimentation and diffusion of spherical particles. These theories were discussed in the preceding paper (Harding & Johnson, 1985). The concentration-dependence of sedimentation is given, correct to first-order in concentration c , by:

$$s_c = s(1 - k_s c) \quad (6)$$

or equivalently:

$$s_c = s(1 - K_s \phi) \quad (7)$$

Here ϕ is the volume fraction ($=cv_s$) and K_s is related to k_s by:

$$K_s = k_s/v_s, \quad (8)$$

v_s being the specific volume (ml/g) of the solvated particle.

A typical plot of s_c versus concentration is given in Fig. 5 (pH 6.8 and 10.10). Plots for the other solvent conditions are similar in form and available from the authors upon request. In several cases, a particular plot contains data obtained on more than one preparation, and evaluations of sedimentation coefficients were performed by different personnel. Good agreement was always observed. The theory of Rowe (1977) provides a value for the sedimentation regression coefficient k_s of $4v_s$, whereas that of Batchelor (1972) gives it as $6.55 v_s$. As discussed previously (Harding & Johnson, 1985), following the work of others (see, e.g., Fujita, 1962), sedimentation coefficients should normally be corrected for solution density rather than solvent density, although no errors are introduced with the latter in

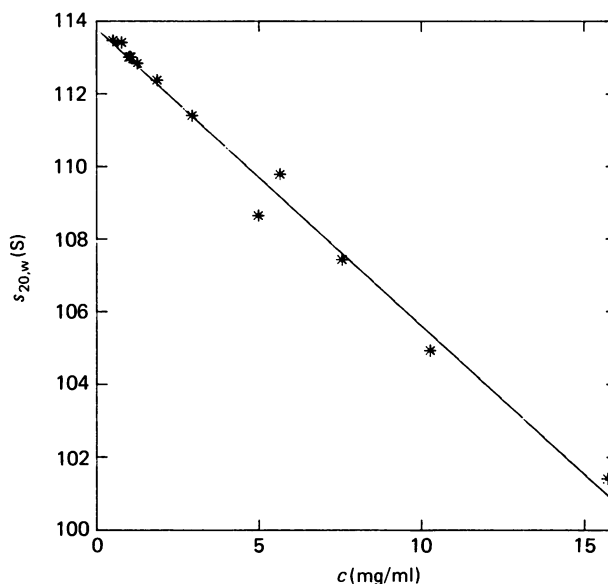


Fig. 5. Plot of sedimentation coefficient versus concentration for TYM virus in phosphate/NaCl buffer, pH 6.8 and 10.10

extrapolation if a consistent convention is used. Batchelor's (1972) coefficient of 6.55 corresponds to the solvent-density convention. Values of k_s and K_s that are corrected for solvent density are denoted respectively by k'_s and K'_s . A simple conversion exists, which can be shown to be exact (see, e.g., Rowe, 1977), for the limiting value of k_s at zero solute concentration:

$$k_s = k'_s - \bar{v} \quad (9)$$

Table 1 also give a comparison of the values for k_s (and k'_s) for the TYM virus solutions in the various solvents. Before any deductions about the theoretical coefficients can be made, values for the parameter v_s are required independently from some other source.

The concentration-dependence of diffusion coefficients provides the basis for one such route. A typical plot is given in Fig. 6 for pH 6.8 and 10.10, and other plots for the other solvent conditions are similar in form. The diffusion coefficient at finite concentration D_c (standardized to water at 20 °C) is related to the diffusion coefficient at zero concentration, D , by:

$$D_c = D(1 + k_D c) \quad (10a)$$

correct to the first order in concentration. k_D is the concentration-dependence diffusion parameter (ml/g) given by Harding & Johnson (1985), as:

$$k_D = 2BM - k'_s \quad (11a)$$

where M is the relative molecular mass and B is the second virial coefficient. Equivalently, writing eqn. (10a) in volume-fraction terms:

$$D_c = D(1 + K_D \phi) \quad (10b)$$

where

$$K_D = (k_D/v_s) = \frac{2BM}{v_s} - K'_s \quad (11b)$$

There are in general at least two contributions to the virial-coefficient term: one from the excluded volume and

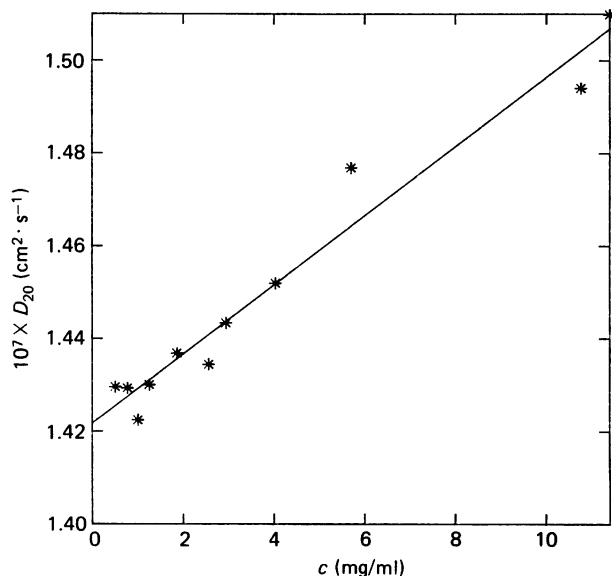


Fig. 6. Plot of diffusion coefficient versus concentration of TYM virus for the same solvent conditions as for Fig. 5

the other(s) from inter-particle forces, in this case probably particle charge effects:

$$B = U/2M^2 + f(Z, I) \quad (12)$$

Here U is the molar excluded volume (ml/mol), and f is a function of the charge, Z , on the macroion and I , the ionic strength. Values for U are available for several simple particle shapes such as spheres, rods and tri-axial ellipsoids (Rallison & Harding, 1985). The charge term $f(Z, I)$ has been given as $Z^2/4I$ [by, e.g., Scatchard (1946) and Ogston & Winzor (1975)] with a correction factor given by Wills *et al.* (1980, eqn. A9). Contributions to eqn. (12) from other solute-solute and solute-solvent interactions are generally taken to be negligible (Ogston & Winzor, 1975; Jeffrey *et al.*, 1977).

In Table 1 are given values of k_D and also values of the second virial coefficient B calculated on the basis of eqn. (11a). It is seen that, after reasonable allowance has been made for experimental error, the B values vary little with solvent condition. As expected, however, there is a slight downward trend in the B values as the pH is lowered towards the isoelectric pH and hence as the charge contribution to B (eqn. 12) approaches zero. B values thus found from sedimentation velocity and diffusion are compared with corresponding values obtained from sedimentation equilibrium as described above. The latter values are only approximate because of the small concentration range employed (the relative molecular mass of TYM virus corresponds to the uppermost limit for this type of experiment). Nonetheless fair agreement is still attained (Table 1).

For a (solvated) spherical particle when charge effects are negligible, the molar excluded volume is related to the (solvated) specific volume by $U/M = 8 v_s$ (Tanford, 1961). Therefore, by using eqn. (12):

$$v_s = BM/4 \quad (13)$$

In Table 1 v_s values thus obtained from B determined in sedimentation velocity/diffusion have been compared. Within experimental error v_s does not vary with experimental conditions. This data were thus used to

Table 3. Comparison of values for K_s (and K'_s)

(a) Determined from the v_s values of Table 1; (b) determined from a v_s of 1.54 ± 0.04 ml/g obtained from eqn. (13b).

$$K_s = k_s/v_s; K'_s = k'_s/v_s$$

Ionic strength was 0.10 except where indicated by an asterisk (*), when it was 0.20.

pH	(a)		(b)	
	$K_s (\pm 0.5)$	$K'_s (\pm 0.5)$	$K_s (\pm 0.4)$	$K'_s (\pm 0.4)$
7.8	5.9	6.3	7.2	7.7
6.8	4.6	5.0	5.2	5.6
6.0	4.7	5.1	5.5	5.9
4.75	4.9	5.3	5.0	5.5
6.8*	4.9	5.3	5.9	6.4

obtain the coefficient K_s (or K'_s) from eqn. (8) (see Table 3). Recalling that the Batchelor (1972) treatment gives $K'_s = 6.55$, it appears that at the highest pH (7.8) experimental support is given. However, for lower pH values the K'_s values (and K_s) are substantially lower.

An estimate for v_s can also be obtained from the relative molecular mass and the equivalent hydrodynamic radius of a Stokes sphere, r_H , by using the relation:

$$v_s = \frac{4\pi N}{3M} \cdot r_H^3 \equiv \frac{1}{162} \cdot \left(\frac{kT}{\pi D}\right)^2 \cdot \frac{(1-\bar{v}\rho)}{s\eta^3} \quad (13b)$$

from eqns. (4) and (5). It is reasonable to assume that, since eqn. (13b) does not involve concentration (and hence charge-dependent) terms (s and D are 'infinite-dilution' values), we may evaluate an effective v_s based on the mean r_H value from Table 2, and on a mean M value from the sedimentation velocity/diffusion M_w values of Table 1. This is 1.54 ± 0.04 ml/g, significantly lower than v_s values appearing in Table 1. The corresponding values of K_s and K'_s given in Table 3(b) are, in general, closer to the values predicted by Batchelor (1972) theory than those appearing in Table 3(a).

We have also used the values of v_s given in Table 1 to obtain a 'thermodynamic' radius, r_B , of the particle, by using the relation:

$$r_B = \sqrt[3]{(3Mv_s/4\pi N)} \equiv \sqrt[3]{(3BM^2/16\pi N)} \quad (14)$$

where N is Avogadro's number. Such values may be compared (Table 2) with the 'hydrodynamic radii' obtained from eqn. (5). Agreement is generally good, notwithstanding the considerable experimental uncertainty introduced in obtaining r_B so indirectly. The values for r_B are, however, consistently higher, particularly at the higher pH values; this is probably indicative of the greater effects of charge on r_B .

For particles of known shape, v_s can be obtained directly from the relation:

$$[\eta] = \nu v_s \quad (15)$$

where ν is the viscosity increment (= 2.5 for spherical particles) and hence, defining R as the ratio of k_s to $[\eta]$, we obtain for spherical particles:

$$R \equiv \frac{k_s}{[\eta]} = \frac{K_s}{2.5} \quad (16)$$

The intrinsic viscosity at pH 6.8 and I 0.10 was found to be 5.3 ± 0.3 . This corresponds to a value of 1.5 for the ratio $k'_s/[\eta]$. This is in good agreement with R values for other spherical and globular particles (see Creeth & Knight, 1965; Harding & Rowe, 1982). Rowe (1977) predicts a value of 1.60 for a spherical particle. The intrinsic viscosity found corresponds to a $k'_s/[\eta]$ ratio of 1.63; this is considerably lower than the predicted value of 2.62 from Batchelor (1972) theory.

In conclusion, our estimates for the concentration-dependence of the transport properties of spherical particles appear reasonably consistent with other empirical observations on latex spheres (Cheng & Schachman, 1955; Maude & Whitmore, 1958; Buscall *et al.*, 1982) although less than the theoretical values predicted by Batchelor (1972), and higher than those expected from Rowe's (1977) treatment. The ratio $k'_s/[\eta]$ appears to be reasonably consistent with the latter model. Batchelor & Wen (1982) have offered an explanation for the results on latex spheres that were lower than expected. They argued that a net attractive (Van der Waal's) force between the particles existed, causing an excess number of close pairs to form, whose sedimentation rate exceeded that of an isolated sphere. A similar explanation is probably applicable to the TYM-virus system.

We thank Mr. D. Reed for expert technical assistance and Dr. P. Witz for the gift of purified TYM virus. We also thank Professor J. M. Kaper for a personal communication of unpublished work. We are grateful for the opportunity of discussing this work with Professor G. K. Batchelor, Dr. J. M. Rallison and Dr. A. J. Rowe. We are indebted to the Oppenheimer Fund for financial support in this work.

REFERENCES

- Batchelor, G. K. (1972) *J. Fluid Mech.* **52**, 245–268
 Batchelor, G. K. & Wen, C. S. (1982) *J. Fluid Mech.* **124**, 495–528
 Buscall, R., Goodwin, J. W. & Ottewill, R. H. (1982) *J. Colloid Interface Sci.* **85**, 78–86
 Cheng, P. Y. & Schachman, H. K. (1955) *J. Polym. Sci.* **16**, 19–30
 Creeth, J. M. & Harding, S. E. (1982a) *J. Biochem. Biophys. Methods* **7**, 25–34
 Creeth, J. M. & Harding, S. E. (1982b) *Biochem. J.* **205**, 635–641
 Creeth, J. M. & Knight, C. G. (1965) *Biochim. Biophys. Acta* **102**, 549–558
 Dawson, R. M. C., Elliot, D. C., Elliot, W. H. & Jones, K. M. (1969) *Data for Biochemical Research*, 2nd edn., p. 487, Clarendon Press, Oxford
 Finch, J. T. & Klug, A. (1966) *J. Mol. Biol.* **15**, 344–364
 Fujita, H. (1962) *Mathematical Theory of Sedimentation Analysis*, chapter 1, Academic Press, New York
 Godfrey, R. E., Johnson, P. & Stanley, C. J. (1982) in *Biomedical Applications of Laser Light Scattering* (Satelle, D. B., Lee, W. I. & Ware, B. R., eds.), pp. 373–389, Elsevier, Amsterdam
 Green, A. A. (1933) *J. Am. Chem. Soc.* **55**, 2331–2336
 Harding, S. E. & Johnson, P. (1984) *Biochem. J.* **220**, 117–123
 Harding, S. E. & Johnson, P. (1985) *Biochem. J.* **231**, 543–547
 Harding, S. E. & Rowe, A. J. (1982) *Int. J. Biol. Macromol.* **4**, 160–164
 Jeffrey, P. D., Nichol, L. W., Turner, D. R. & Winzor, D. J. (1977) *J. Phys. Chem.* **81**, 776–781
 Kaper, J. M. (1960a) *Nature (London)* **160**, 219–220
 Kaper, J. M. (1960b) *J. Mol. Biol.* **2**, 425–433
 Kaper, J. M. (1975) *The Chemical Basis of Virus Structure, Dissociation and Reassembly*, pp. 157–158, North-Holland, Amsterdam
 Kaper, J. M. & Litjens, E. C. (1966) *Biochemistry* **5**, 1612–1617
 Klug, A. & Finch, J. T. (1960) *J. Mol. Biol.* **2**, 201–215
 Klug, A., Longley, W. & Leberman, R. (1966) *J. Mol. Biol.* **15**, 315–343
 Markham, R. (1951) *Discuss. Faraday Soc.* **11**, 221–227
 Maude, A. D. & Whitmore, R. L. (1958) *Br. J. Appl. Phys.* **9**, 477–482
 Nureddin, A. & Johnson, P. (1977) *Biochemistry* **16**, 1730–1737
 Ogston, A. G. & Winzor, D. J. (1975) *J. Phys. Chem.* **79**, 2496–2500
 Pusey, P. N. (1974) in *Photon Correlation and Light Beating Spectroscopy* (Cummins, H. Z. & Pike, E. R., eds.), p. 387, Plenum Press, New York
 Rallison, J. M. & Harding, S. E. (1985) *J. Colloid Interface Sci.* **103**, 284–289
 Ross, P. D. & Minton, A. P. (1977) *J. Mol. Biol.* **112**, 437–452
 Rossman, M. G. (1984) *Biochem. Soc. Trans.* **12**, 115–126
 Rowe, A. J. (1977) *Biopolymers* **16**, 2595–2611
 Sanders, A. H. & Cannell, D. S. (1980) in *Light Scattering in Liquids and Macromolecular Solutions* (Degiorgio, V., Corti, M. & Giglio, M., eds.), pp. 173–182, Plenum Press, New York
 Scatchard, G. (1946) *J. Am. Chem. Soc.* **68**, 2315–2319
 Svedberg, T. & Pedersen, K. O. (1940) *The Ultracentrifuge*, pp. 20–22, Oxford University Press, Oxford
 Szuchet-Derechin, S. & Johnson, P. (1966) *Eur. Polym. J.* **2**, 115–128
 Tanford, C. (1955a) *J. Phys. Chem.* **59**, 798–799
 Tanford, C. (1955b) in *Electrochemistry in Biology and Medicine* (Shedlovsky, T., ed.), pp. 248–265, John Wiley and Sons, New York
 Tanford, C. (1961) *Physical Chemistry of Macromolecules*, pp. 195–196, 234, John Wiley and Sons, New York
 Teller, D. C. (1973) *Methods Enzymol.* **27**, 346–441
 Wills, P. R., Nichol, L. W. & Siezen, R. J. (1980) *Biophys. Chem.* **11**, 71–82

Received 12 February 1985/31 May 1985; accepted 27 June 1985